Systematic Uncertainties in Theoretical Predictions of Jet Quenching

W. A. Horowitz*
Physics Department, The Ohio State University,
191 West Woodruff Avenue, Columbus, OH 43210, USA

B. A. Cole†
Physics Department, Columbia University,
538 West 120th Street, New York, NY 10027, USA

(Dated: October 9, 2009)

We find that the current radiative energy loss kernels obtained from the opacity expansion dramatically violate the collinear approximation used in their derivation. By keeping only the lowest order in collinearity terms, models based on the opacity expansion have $\sim 50\%$ systematic uncertainty in the calculation of π^0 R_{AA} in 0-5% most central RHIC collisions resulting in a systematic uncertainty of $\sim 200\%$ in the extracted medium density. Surprisingly, the inclusion of a thermal gluon mass on the order of the Debye screening scale affects R_{AA} at only about the 5% level due to non-intuitive coherence effects. For some observables such as R_{AA}, the effect of these uncertainties decreases with increasing jet energy; for others, such as the average number of radiated gluons, the effect is energy independent. We note that it is likely that the differences reported in the extracted values of medium parameters such as $\hat{q}$ by various jet energy loss models will fall within this collinear approximation systematic uncertainty; it is imperative for the quantitative extraction of medium parameters or the possible falsification of the hypothesis of weak coupling between the hard probes and soft modes of the quark gluon plasma medium that future radiative energy loss research push beyond the lowest order collinear approximation.

PACS numbers: 12.38.Mh, 24.85.+p, 25.75.-q
Keywords: QCD, Relativistic heavy-ion collisions, Quark gluon plasma, Jet quenching

I. INTRODUCTION

Jet quenching is a unique observable in ultra-relativistic heavy ion collisions (URHIC) as high transverse momentum (high-p_T) particles are the most controlled, calibrated, and direct probe of the fundamental soft degrees of freedom of the quark-gluon plasma (QGP) [1]. Rigorous falsification or confirmation of fundamentally different qualitative pictures of the basic physics of the QGP (e.g., whether it is strongly or weakly coupled [2], its relevant degrees of freedom [3–5], etc.) from comparing theoretical predictions to high-p_T data crucially requires a detailed understanding of both experimental *and theoretical* uncertainties.

Once the qualitative picture is fixed, jet tomography [6, 7], the *quantitative* determination of bulk properties of the QGP through the study of the attenuation pattern of high momentum particles, becomes possible. Jet tomography requires both high precision experimental data and a precise theoretical understanding of partonic energy loss. Recent statistical analyses by PHENIX [8, 9] assuming infinite precision for theoretical calculations that assume a weakly-coupled QGP suggest that data are now certain enough to extract medium properties to within $\sim 20\%$. Given that no current perturbative energy loss model satisfactorily and simultaneously describes more than one high-p_T observable [10, 11], such as the level of suppression and azimuthal anisotropy of the high-p_T gluons, light quarks, and heavy quarks as measured through the light meson [12–15] and non-photonic electron nuclear modification factor [16–19], $R_{AA}(p_T, \phi)$, and the away-side suppression of jet-triggered hadrons, I_{AA} [20], it is, perhaps, premature to claim that even a qualitative understanding of the jet quenching of the QGP exists.

x:	x_+		$x_+(x_E)$	x_E	
$\theta_{\max}$:	$\pi/2$				$\pi/4$
m_g:	$\mu/\sqrt{2}$	0			
Rad Only dN_g/dy ($\times$ 1000)	$3.0^{+0.7}_{-0.5}$	$2.4^{+0.5}_{-0.4}$	$2.0^{+0.4}_{-0.3}$	$4.0^{+0.9}_{-0.6}$	$5.9^{+1.1}_{-1.0}$
Rad+El dN_g/dy ($\times$ 1000)	$1.0^{+0.3}_{-0.1}$	$1.0^{+0.2}_{-0.2}$	$0.9^{+0.2}_{-0.2}$	$1.3^{+0.2}_{-0.2}$	$1.5^{+0.3}_{-0.3}$

TABLE I: Comparison of the extracted dN_g/dy for the work considered here compared to PHENIX 0-5% most central π^0 data. Note especially the nearly factor of 3 difference in the last three columns when using Rad Only (radiative energy loss only). Due to the use of the collinear approximation all three of these values should be considered equally valid determinations of the medium density. The assumed infinite precision for the elastic channel makes the convolved Rad+El extraction of dN_g/dy suffer a smaller systematic uncertainty than from those studied in the radiative channel alone. The first two columns demonstrate the limited influence of the radiated gluon mass in measuring the medium density. See the text for more details.

*Electronic address: horowitz@mps.ohio-state.edu
†Electronic address: cole@nevis.columbia.edu

Nevertheless, continuing with the assumption that the current perturbative quantum chromodynamics (pQCD) models accurately describe the physics, such quantitative extractions of medium properties can only be meaningful when the systematic uncertainties in the theoretical calculations and modeling are both known and included in the systematic uncertainties in the extracted quantities. While there have been some previous qualitative estimates of the theoretical uncertainty stemming from the running of the strong coupling [21, 22], the probability leakage of the Poisson convolution [23, 24], and a phenomenological IR cutoff imposed to approximate the effects of a non-zero thermal gluon mass [25], one of the main purposes of this paper is to begin the process of rigorously quantifying the combined experimental uncertainties and systematic theoretical uncertainties in extracted medium parameters.

In particular, we investigate the theoretical uncertainties due to the collinear approximation and due to different assumptions regarding the thermal mass of the radiated gluon in the opacity expansion approach [26–30] for calculating the radiative energy loss of high-p_T partons in pQCD. We also asses how those uncertainties change when elastic energy loss is included [31, 32]. A summary of our results is shown in Table I. Most strikingly, we find that keeping only the lowest order term in collinearity results in $\sim 200\%$ systematic uncertainty on the value of the extracted gluon rapidity density for central Au+Au collisions at top RHIC energies. While this paper does not quantify the uncertainties associated with the collinear approximation for other pQCD radiative energy loss models, [23, 26, 33, 34], the uncertainties in those models are almost certainly similar to the results quoted here. In particular, the sizable discrepancies between the extracted medium properties by different energy loss groups [8, 9, 35] are probably within the current theoretical systematic uncertainty.

There are, generally speaking, four main pQCD-based radiative energy loss formalisms applied to URHIC: opacity expansion (GLV) [7, 26, 27, 29, 30], multiple soft scattering (BDMPS-Z-ASW) [28, 36–45], higher-twist (HT) [46–49], and thermal field theory (AMY) [50–53]. In this work we focus quantitatively on the opacity expansion approach; see Fig. 1 for a cartoon of the physics involved and visualizations of the key variables discussed in this text. Within the GLV formalism one derives an expression for the single inclusive radiated gluon spectrum, dN_g/dx, that is folded into a Poisson convolution [7] for the distribution of total radiated energy by the parent parton (see below). Like all radiative energy loss models, the formalism makes the eikonal approximation, namely that the parent parton has a sufficiently high energy that its path is approximately straight and that the interference from the away-side jet, of $\mathcal{O}(1/E)$, may be safely ignored [54]. The formalism also neglects contributions from four-gluon vertices and assumes that the parent parton suffers independent, path-ordered collisions. These choices are justified in the opacity expansion approach by

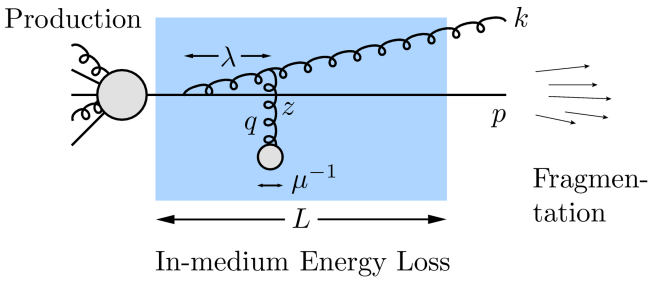

FIG. 1: (Color online) Cartoon of the production, in-medium energy loss, and fragmentation processes that may occur perturbatively for a high-p_T parton produced in a heavy ion collision. The momentum labels are p for the outgoing parent parton, k for the medium-induced bremsstrahlung gluon, and q for the momentum transfer between an in-medium soft degree of freedom and the high-p_T parent parton. Note the ordering of length scales displayed, $\mu^{-1} \ll \lambda \ll L$.

the assumption of a medium composed of Debye-screened scattering centers whose screening length $\mu^{-1} \ll \lambda$ is much smaller than the mean free path of the parent parton [36]. Such an ordering of scales is consistent with thermal field theoretic estimates for μ and λ [55].

Current evaluations of the diagrams resulting from the opacity expansion formalism drop a significant number of terms that are assumed to be small. These approximations were made for analytic simplicity, but they do not seem to be inherently required. Specifically, GLV takes: (1) the collinear approximation, $k_T \ll xE$, where k is the momentum of the radiated gluon and k_T its component transverse to the motion of the parent parton; (2) the parent parton path length much longer than the gluon mean free path, $L \gg \lambda$; and (3) the soft radiation limit, $x \ll 1$, where x is the momentum fraction taken away by the radiated gluon (discussed further below). We note that all these assumptions are also made in the BDMPS and AMY formalisms[1]. HT makes a similar assumption to (2), does not make the soft gluon approximation (3), but does assume collinearity (1). After discussing (1) in greater detail we will briefly touch on (2) and (3) further below.

This work focuses on the collinear approximation, $k_T \ll xE$, and, more generally, the effects of limiting the phase space into which gluon bremsstrahlung is allowed to radiate. The current derivations using the opacity expansion formalism yield a single inclusive gluon ra-

[1] In GLV and BDMPS (2) is used to neglect poles from propagators multiplied by $\exp(-\mu\Delta z) \approx \exp(-\mu\lambda) \ll 1$, where Δz is the distance between successive scattering centers; this approach is probably invalid for $L \lesssim \lambda \sim 1$ fm. On the other hand AMY uses the central limit theorem in its Langevin approach and corrections are likely for $L \lesssim 30\lambda \sim 30$ fm; this extra long path length is also required by the neglect of the interference between vacuum and in-medium induced radiation.

diation kernel, $dN_g/dxdk_T$, that knows nothing about the approximations used in its derivation; in calculating dN_g/dx the collinear approximation is enforced phenomenologically with a UV cutoff in the k_T integration. We find that the $dN_g/dxdk_T$ kernel maximally violates the assumption of collinearity at small x. It is not surprising, therefore, that dN_g/dx, and observables dependent on it such as R_{AA}, are highly sensitive to the $\mathcal{O}(1)$ variations of the cutoff one explores in estimating a systematic theoretical uncertainty. Even worse, as we discuss further below, the use of only the lowest order collinear term means that collinearly equivalent definitions of x yield values of medium density extracted from data that differ by $\sim 100\%$.

Previous work [25] that investigated a phenomenological k_T cutoff in the IR to approximate a thermal mass of the radiated gluon found a similarly strong sensitivity to the specifics of the cutoff. However, we find that with an explicit derivation of energy loss for non-zero gluon mass instead of a cutoff imposed by hand *a posteriori*, surprising and non-trivial cancellations yield an energy loss that has little sensitivity to the exact value of m_g.

II. OTHER SOURCES OF UNCERTAINTY

Before returning to the primary focus of the paper—uncertainties introduced by the collinear approximation—it is worth enumerating here other potential sources of theoretical uncertainty that we do not attempt to quantify in this work but that, nonetheless, could be quite large.

In this paper, we calculate radiative energy loss using the first order expression from the opacity expansion; i.e. the single inclusive gluon radiation spectrum is derived by scaling up diagrams with only a single in-medium scattering for the parent parton or its bremsstrahlung radiation, as is depicted in Fig. 1, by the average number of scatterings, L/λ. The n^{th} order in opacity explicitly evaluates the interference terms, neglected in the lower order expressions, from diagrams with n in-medium scatterings. Within the set of approximations given above, and assuming the medium consists of Debye-screened static scattering centers, the GLV formalism yields a closed form expression for dN_g/dx to all orders in opacity. Numerical study of dN_g/dx [7, 27, 55] suggests that it does receive corrections from higher orders but that these are relatively small—around the $\sim 30\%$ level for relatively long paths of $L = 5$ fm and smaller for shorter paths—for RHIC- and LHC-like conditions.

The Poisson convolution [7, 36] of the dN_g/dx kernel is an attempt to approximate the full probability distribution of radiative energy loss, $P(\epsilon)$, where the fraction of radiated energy is defined by $E_f = (1-\epsilon)E_i$. The convolution assumes independent, incoherent emission of gluons; the effect of neglecting the interference between two or more emitted gluons is not currently known. There are also uncertainties associated with "probability leakage" [7, 23]: in model implementations the parent parton energy is often not dynamically updated throughout the convolution leading to the possible violation of energy conservation (i.e. $P(\epsilon)$ has support for $\epsilon > 1$). In this work, we assign the total weight from the convolution at $\epsilon > 1$ to a delta function centered at $\epsilon = 1$ (complete stopping), the so-called "non–re-weighted" approach [23]. Studies have shown that this procedure reproduces reasonably well distributions obtained from Poisson convolution procedures that dynamically update the parent parton energy [56]. Moreover, for energy loss calculations based on the GLV formalism, the leakage tends to be small. When elastic energy loss is included this leakage is even smaller [57].

A realistic model of jet quenching in URHIC requires a weighted averaging over a large range of medium path lengths $0 \lesssim L \lesssim 12$ fm. QGP temperatures at RHIC energies lead to a gluonic mean free path of $\lambda \sim 1-2$ fm [55]. Additionally, even in the most central collisions, a significant portion of path lengths have $L \lesssim 2$ fm, and the bias towards the surface from energy loss makes these shorter paths even more important [23, 32]. The assumption, $L \gg \lambda$, is therefore violated for a large fraction of energy loss inducing processes. In the R_{AA} calculations of this work, we simply apply the GLV formalism to all path lengths. There is an additional uncertainty associated with mapping the realistic medium density of heavy ion collisions—with its approximate Bjorken expansion and non-trivial, time-dependent transverse density profile—into the static, uniform "brick" problem in which the analytic formulae were derived.

The small x approximation seems reasonable at RHIC energies where the single inclusive gluon radiation spectrum dN_g/dx peaks at $x \sim \mu/E \lesssim 0.05 \ll 1$. The small-$x$ approximation should apply even better at LHC, where E will be larger by a factor ~ 10. However, the Poisson convolution widens the original dN_g/dx spectrum—no matter how low the x value of the peak of the spectrum—thus distributing its weight out to larger values x. In this way the convolution introduces a sensitivity to the large x region of dN_g/dx that is not well controlled due to the $x \ll 1$ assumption.

Probably the largest source of uncertainty, likely bigger even than that due to the collinear approximation that we detail in this paper, will result from values chosen for and/or the running of α_s [21, 22]; since radiative energy loss varies as α_s^3, it is highly sensitive to changes in the value of the coupling. One factor of α_s arises from the emission of the gluon bremsstrahlung while the other two result from interacting with the soft degrees of freedom in the medium; see Fig. 1. For these last two couplings it is not even clear what scale should be chosen for the running. Nevertheless, the momentum transfer q will always probe soft scales on the order of $\mu \sim 0.5$ GeV $\gtrsim \Lambda_{\text{QCD}} \sim 0.2$ GeV, and non-perturbative physics will be involved. The lack of a proof of factorization, whereby these non-perturbative contributions necessarily become small at high energies, is of course not particularly com-

forting.

III. OPACITY EXPANSION ENERGY LOSS KERNEL AND x

The first order in opacity result for the radiated gluon spectrum assuming massive quarks and gluons and using the Gyulassy-Wang model of static scattering centers [3], to lowest order in x and k_T/xE, where $k_T = |\mathbf{k}|$, is given by [29]

$$x\frac{dN_g}{dx} = \frac{C_R\alpha_s}{\pi}\frac{L}{\lambda}\int\frac{d^2\mathbf{q}}{\pi}\frac{2d^2\mathbf{k}}{\pi}\frac{\mu^2}{\left(\mathbf{q}^2+\mu^2\right)^2} \times\frac{\mathbf{k}\cdot\mathbf{q}(\mathbf{k}-\mathbf{q})^2-\beta^2\mathbf{q}\cdot(\mathbf{k}-\mathbf{q})}{\left[(\mathbf{k}-\mathbf{q})^2+\beta^2\right]^2\left(\mathbf{k}^2+\beta^2\right)} \times\int dz\left[1-\cos\left(\frac{(\mathbf{k}-\mathbf{q})^2+\beta^2}{2Ex}z\right)\right]\rho(z). \quad (1)$$

Here, $\beta^2 = x^2M^2+m_g^2$, where M is the mass of the parent parton, and m_g is the mass of the radiated gluon; $C_R = C_F$ for a parent quark, and $C_R = C_A$ for a parent gluon. The corresponding result for massless parent quarks/gluons and/or massless radiated gluons is obtained by setting M and/or m_g to zero in Eq. (1), respectively. After temporarily taking the $q_T = |\mathbf{q}|$ medium exchange momentum limit to infinity and making a change of variables (see [29] for more details) and additionally assuming an exponentially decaying distribution, $\rho(z)$, for the distance to the scattering center[2], Eq. (1) becomes

$$\frac{dN_g}{dx} = \frac{8C_R\alpha_s\mu^2}{\pi\,x}\frac{L}{\lambda}\int dq_T dk_T\frac{q_T^3}{(4xE/L)^2+(q_T^2+\beta^2)^2} \times\frac{k_T}{k_T^2+\beta^2}\frac{k_T^2(k_T^2+\mu^2-q_T^2)+\beta^2(q_T^2+\mu^2-k_T^2)}{\left((k_T-q_T)^2+\mu^2\right)^{3/2}\left((k_T+q_T)^2+\mu^2\right)^{3/2}}. \quad (2)$$

We note that supposing the scattering center distribution to be uniform instead of exponentially decaying appears to make only a small difference in the gluon spectrum [57].

The integrand in Eq. (2) is both IR and UV safe. In principle, we could set the lower and upper q_T and k_T limits of integration to 0 and ∞, respectively. If the integrand were exact, then it would have support only in the physical regions of the q_T and k_T integration space.

[2] In general it is necessary to specify the distribution in the *difference* in distance between successive scattering centers. In the first order in opacity case, with only one scattering center, this difference in distance is between the scattering center and the production point. One can always take the production point to be at $z = 0$, and thus in this case the specified distribution is the distance to the first scattering center.

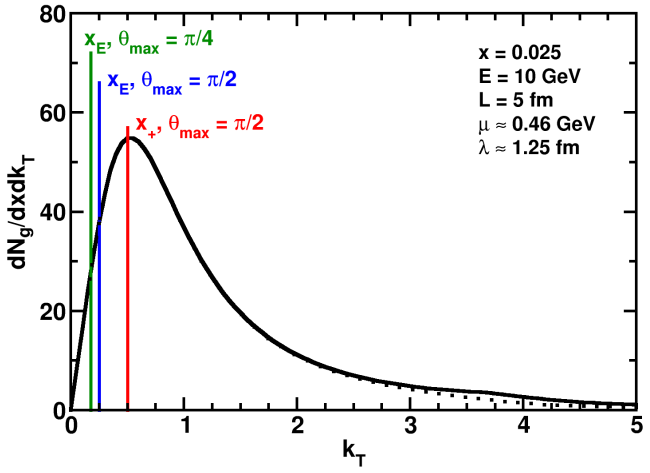

FIG. 2: Plot of $dN_g/dxdk_T$ from Eq. (2) (solid curve) for a light quark with all masses set to 0, $E = 10$ GeV, $L = 5$ fm, and representative values of $\mu \simeq 0.46$ GeV and $\lambda \simeq 1.25$ fm for a medium density of $dN_g/dy = 1000$ similar to RHIC conditions [32]. Vertical lines depict the values of k_T used as cutoffs to enforce collinearity in Eq. (2). Note that with $x = 0.025 \sim \mu/E$, $dN_g/dxdk_T$ is large near $k_T \sim k_{\max}$, completely in contradiction with the collinear approximation. Dotted curve, from the unshifted integrand of Eq. (1), differs only slightly from the spectrum obtained from the shifted integrand of Eq. (2) (solid curve).

However, due to the small x and collinear approximations, the integrand violates kinematic limits: one can clearly see that the integrand in Eq. (2) has support over all q_T and k_T (this is also true of the unshifted integrand, Eq. (1)). We enforce physicality in the hope of better approximating the exact result by restricting the q_T and k_T integration region with cutoffs. A new result from this paper is a quantitative estimate of the systematic error that results from allowing $\mathcal{O}(1)$ variations of these cutoffs on some observables and extracted medium parameters. Surprisingly, we find that dN_g/dx is highly sensitive to variations in the k_T UV cutoff.

For the q_T integration we will make the usual choices $q_{\min} = 0$ and $q_{\max} = \sqrt{3\mu E}$. The value for $q_{\max}$ is, in principle, the maximum momentum transfer allowed using relativistic kinematics, though it has been pointed out that this is no longer correct with the change of variables $\mathbf{q} \to \mathbf{q}+\mathbf{k}$ used in the final steps leading to Eq. (2)[3]. Nevertheless, Eq. (2) is rather insensitive to the q_T cutoff [29], and we show below explicit calculations of $dN_g/dxdk_T$ using the shifted and unshifted integrands of Eqs. (2) and (1), respectively. These comparisons in Figs. 2 and 3 demonstrate that the shifted integrand with the unshifted $q_{\max}$ well reproduces the results of the unshifted integrand, albeit with minor artifacts.

Previous work by BDMS [25] found a strong sensitivity

[3] We thank Ulrich Heinz for finding this error in logic.

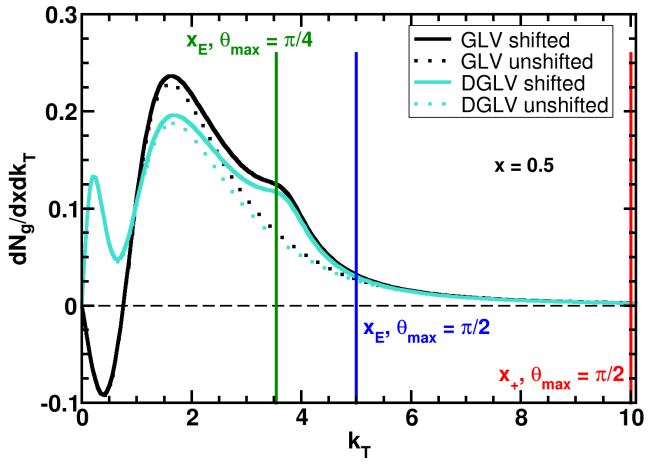

FIG. 3: Comparison of $dN_g/dxdk_T$ spectra as a function of k_T with $x = 0.5$ between GLV (all masses set to zero) and DGLV (non-zero radiated gluon mass) formulations using both the shifted integrand of Eq. (2) (solid curves) and the unshifted integrand of Eq. (1) (dotted curves). The horizontal dashed line at 0 is meant to guide the eye. The three vertical lines represent the choices of $k_{\max}$ described in the text. $dN_g/dxdk_T$ better respects the collinear approximation for larger values of x as it has little weight near $k_T \sim k_{\max}$. At small k_T the radiated gluon mass, surprisingly, *enhances* radiation for DGLV due to coherence effects; at larger k_T the mass has the expected effect of suppressing $dN_g/dxdk_T$.

to a phenomenological IR cutoff in the k_T integration of the BDMPS multiple soft scattering calculation, a residual of the original vacuum radiation IR divergence. They also showed that the sensitivity of a quenching factor to variations in this cutoff decreased with increasing parent parton energy. The IR cutoff was imposed in order to approximate the influence of a non-zero thermal gluon mass; we find that including a gluon mass at the level of the gluon propagators [29] decreases the sensitivity of the energy loss and calculated R_{AA} (see Table I) to the choice of gluon mass. This result is due to a non-trivial cancellation of effects that we will discuss further below.

We do find, however, that the radiated gluon spectrum and resulting parton energy loss are extremely sensitive to the choice of the UV cutoff in the k_T integration. Furthermore we find a sensitivity to the particular interpretation of x used in relating the components of k to the components of p. It turns out that the derivations of dN_g/dx in the literature have used two different, albeit equal to lowest order in collinearity, definitions of x. We will use the light-cone normalization $p^{\pm} = p^0 \pm p^z$, with inverse $p^{0,z} = (p^+ \pm p^-)/2$, and denote $p^0 = E$ and $p^+ = E^+$. With these conventions the two definitions of x are: (1) the fraction of plus momentum carried away by the gluon, $x = x_+ \equiv k^+/E^+$ [26, 27]; and (2) the fraction of energy carried away by the gluon, $x = x_E \equiv k^0/E$ [28]. In the usual notation where parentheses designate four-momenta, $k = (k^0, k^z, \mathbf{k})$, square brackets light-cone momenta, $k = [k^+, k^-, \mathbf{k}]$, and bold-faced variables are the transverse 2-vectors ($k_T = |\mathbf{k}|$), we find that the radiated massless gluon has on-shell momentum

$$k = (x_E E,\ \sqrt{(x_E E)^2 - \mathbf{k}^2},\ \mathbf{k}) = [x_+ E^+,\ \frac{\mathbf{k}^2}{x_+ E^+},\ \mathbf{k}]. \tag{3}$$

With these definitions of x_+ and x_E one may derive the exact relationships

$$x_+ = \frac{1}{2}\, x_E \left(1 + \sqrt{1 - \left(\frac{k_T}{x_E E}\right)^2}\right), \tag{4}$$

$$x_E = x_+ \left(1 + \left(\frac{k_T}{x_+ E^+}\right)^2\right), \tag{5}$$

where we have assumed that the initial parent parton momentum is $P = (E, E, \mathbf{0})$, and, hence, $E^+ = 2E$. From these formulas, it is easy to see that in the the collinear limit, $x_+ = x_E$, so it is natural that the integrand in Eq. (2) is the same when derived using these two different definitions of x: in one case terms of order $k_T/x_E E$ are dropped whereas in the other terms of order $k_T/x_+ E^+$ are dropped. Thus $dN_g/dx_+ dk_T dq_T(x_+) = dN_g/dx_E dk_T dq_T(x_E)$ in the collinear limit.

Two justifications for and derivations of a k_T cutoff exist in the literature: (1) when interpreting x as x_E, $k_{\max} = x_E E$ keeps k always real (note that in the $x = x_+$ representation k is real regardless of the value of k_T) [43]; (2) when interpreting x as x_+, $k_{\max} = x_+ E^+$ enforces forward emission ($k^+ \geq k^-$) [58][4]. In this work, we will interpret $k_{\max}$ as enforcing consistency with the collinear approximation. It is, then, useful to determine that cutoff from a physical condition independent of the interpretation of x; we choose to set $k_{\max}$ by requiring the emitted radiation be within a cone of angle $\theta_{\max}$ centered on the direction of the parent parton. In this way we may control the collinearity of the radiation by varying the maximum angle of emission allowed. Simple trigonometry relates

$$k_{\max} = \begin{cases} x_+ E^+ \tan(\theta_{\max}/2), & x = x_+, \\ x_E E \sin(\theta_{\max}), & x = x_E. \end{cases} \tag{6}$$

In particular, when $\theta_{\max} = \pi/2$

$$k_{\max} = \begin{cases} x_+ E^+ = 2x_+ E, & x = x_+, \\ x_E E, & x = x_E, \end{cases} \tag{7}$$

and we see that the two original justifications of the $k_{\max}$ cutoff are manifestations of the same physical condition,

[4] An even more restrictive cutoff for k_T results if one also requires forward propagation of the parent parton [7]. Surprisingly this tighter cutoff, which forbids support for dN/dx for $x > 1$ and therefore enforces energy conservation, leads to only a small change in dN_g/dx [57], and we will not use it here.

Name	x	Jacobian	$\theta_{\rm max}$	m_g
x_+, $m_g = \mu/\sqrt{2}$	x_+	No	$\pi/2$	$\mu/\sqrt{2}$
x_+, $m_g = 0$	x_+	No	$\pi/2$	0
$x_+(x_E)$, $\theta_{\rm max} = \pi/2$	x_+	Yes	$\pi/2$	0
x_E, $\theta_{\rm max} = \pi/2$	x_E	No	$\pi/2$	0
x_E, $\theta_{\rm max} = \pi/4$	x_E	No	$\pi/4$	0

TABLE II: Descriptions of the five main radiative energy loss implementations investigated in this work and their names when listed in diagrams. See the text for details.

namely forward emission. It is worth emphasizing that with $k_{\rm max}$ given by Eq. (7), for any numerically equal value of x_+ and x_E the integrand in Eq. (2) is integrated out twice as far in k_T when interpreting x as x_+ as opposed to interpreting x as x_E. We note that a previous study [44] also varied the upper limit of the k_T integration. However that work investigated the radiation into jet cones of various sizes; here we are interested in quantifying the impact of regions of k_T space over which there is currently little or no theoretical control.

If the integrand of Eq. (2) respected the assumptions that went into its derivation over the entire integration region, then it would have little weight for $k_T \sim xE$. However, Fig. 2 shows that there are values of x for which $dN_g/dxdk_T$ has large contributions from $k_T \sim xE$. In fact, we should expect such a result: the Debye mass μ is the natural scale for k_T, and $dN_g/dxdk_T$ will always have a significant weight at $k_T \sim \mu$. As a result, varying $k_{\rm max} \sim xE$ will always lead to large changes in dN_g/dx near $x \sim \mu/E$. In the kinematic regime relevant for RHIC and LHC, numerical study suggests that (1) $dN_g/dx(x)$ reaches its maximum at $x \sim \mu/E$ and (2) $dN_g/dxdk_T(x \sim \mu/E, k_T)$ reaches its maximum at $k_T \sim k_{\rm max}$; for $x \sim \mu/E$ the maximum value of dN_g/dx rises quadratically with $k_{\rm max}$. These observations imply a dramatic sensitivity of dN_g/dx—and any quantities derived from it—to the precise choice of $k_{\rm max}$. Increasing the radiating parton energy decreases the region of x over which dN_g/dx is highly sensitive to the cutoff, $x \lesssim \mu/E$. Naively, then, one might expect that increasing E would decrease the sensitivity of observables calculated from dN_g/dx to variations of $k_{\rm max}$. However, we will show below that even this expectation does not generally hold.

Fig. 3 shows that, as expected, as x increases the assumption of collinearity, $k_T \ll xE$, becomes a better approximation: $dN_g/dxdk_T$ has little weight near $k_T \sim k_{\rm max}$, and, therefore, for these larger values of x dN_g/dx has less sensitivity to the exact choice of $k_{\rm max}$. One may also observe in the figure the negative values of $dN_g/dxdk_T$ for the massless case at small values of k_T. These negative values are due to the destructive interference between the $0^{\rm th}$ order vacuum production radiation (the QCD analog of the usual beta-decay radiation spectrum from QED) and the $1^{\rm st}$ order medium-induced radiation. The interference is controlled by the ratio of the radiating parton path length L and the coherence length,

$$\tau_{\rm coh} = \frac{2xE}{q_T^2 + \beta^2} \tag{8}$$

found by examining the cosine term in Eq. (2) (q_T enters $\tau_{\rm coh}$ here due to the shift in integration variables $q_T \to q_T + k_T$ in going from Eq. (1) to Eq. (2)). For larger values of x the coherence length, $\tau_{\rm coh}$ is longer, and the destructive interference more important; hence $dN_g/dxdk_T$ is negative for small values of k_T for the massless results shown in Fig. 3 but not in Fig. 2. Including a non-zero mass for the radiated gluon reduces $\tau_{\rm coh}$ and therefore the influence of the destructive interference. As a result, for small values of k_T the $dN_g/dxdk_T$ spectrum is actually *enhanced* for the massive as compared to massless case. At larger values of k_T the non-zero thermal gluon mass exhibits the expected effect of suppressing bremsstrahlung radiation. Unfortunately, then, introducing a phenomenological k_T cutoff in the IR into a massless dN_g/dx formula does not capture well the complicated dynamics resulting from allowing the radiated gluons to pick up a non-zero thermal mass from the medium. More readily visible in Fig. 3 than in Fig. 2 is the removal of the minor artifacts from the shift in integration variable when evaluating the unshifted integrand of Eq. (1).

The ambiguity in the interpretation of x has consequences beyond the differences in the corresponding limits of the k_T integration. The gluon dN_g/dx distributions obtained from Eq. 2 using the two different x definitions imply different gluon energy spectra and, thus, different amounts of jet quenching. These differences will clearly contribute to the systematic uncertainty in the interpretation of experimental data using the opacity expansion formalism and any other energy loss formalism that invokes the same or similar collinear approximations. Furthermore, in order to better understand the consequences of the different physical pictures used in different formalisms—e.g. by comparing the gluon spectra produced by GLV (traditionally interpreting x as x_+) and BDMPS-Z-ASW (x as x_E)—one wants all results in terms of the same variables. As a first step we will examine an "apples-to-apples" comparison between results derived from the two interpretations of x solely within the opacity expansion approach.

There is an additional problem with energy loss calculations that interpret x in Eq. (2) as x_+: evaluation of the Poisson convolution $P(\epsilon)$, where ϵ is explicitly an *energy* fraction. Previous models that assumed the x_+ interpretation in dN_g/dx invoked the collinear approximation in order to directly use $dN_g/dx_+(x_+)$ unmodified as the input for the Poisson convolution. As we have shown this is a poor assumption.

In order to compare the two interpretations of x within GLV and to quantify the effect of assuming $dN_g/dx_+ \approx dN_g/dx_E$ in finding $P(\epsilon)$ we need to transform $dN_g/dx_+(x_+)$ to $dN_g/dx_E(x_E)$, which requires the

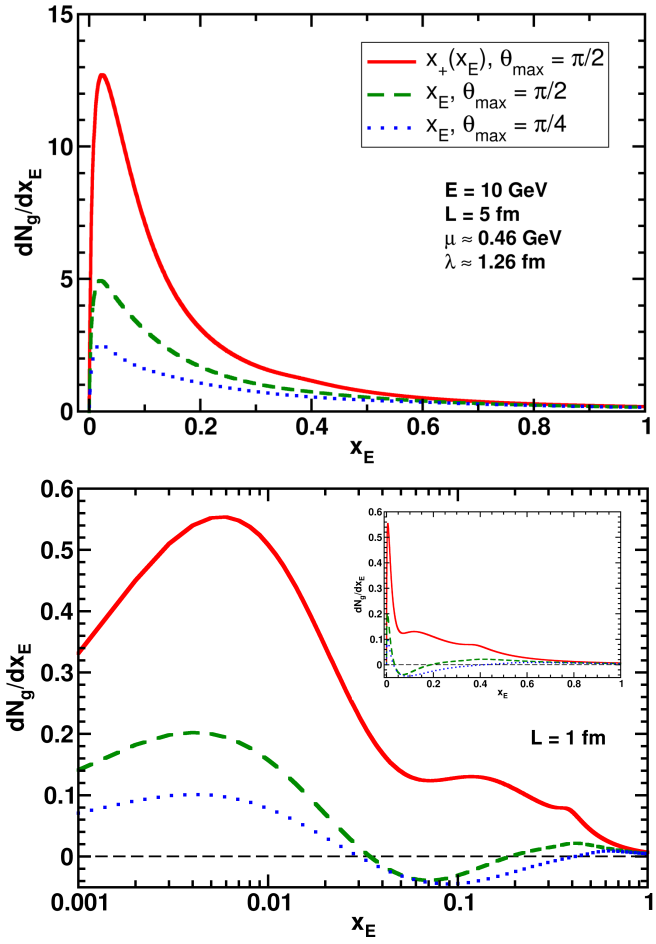

FIG. 4: Comparison of $dN_g/dx_E(x_E)$ for a 10 GeV quark using typical RHIC medium parameters and $L = 5$ fm (top), $L = 1$ fm (bottom) for the collinearly equivalent expressions dN_g/dx from Eq. (2) with the $x = x_E$ interpretation and $x_+(x_E)$ from Eq. (9). Also shown is dN_g/dx from Eq. (2) with $x = x_E$ and $\theta_{\max} = \pi/4$ in order to explore the systematic uncertainty in the choice of $k_{\max}$. Inset shows results on a linear scale for clarity.

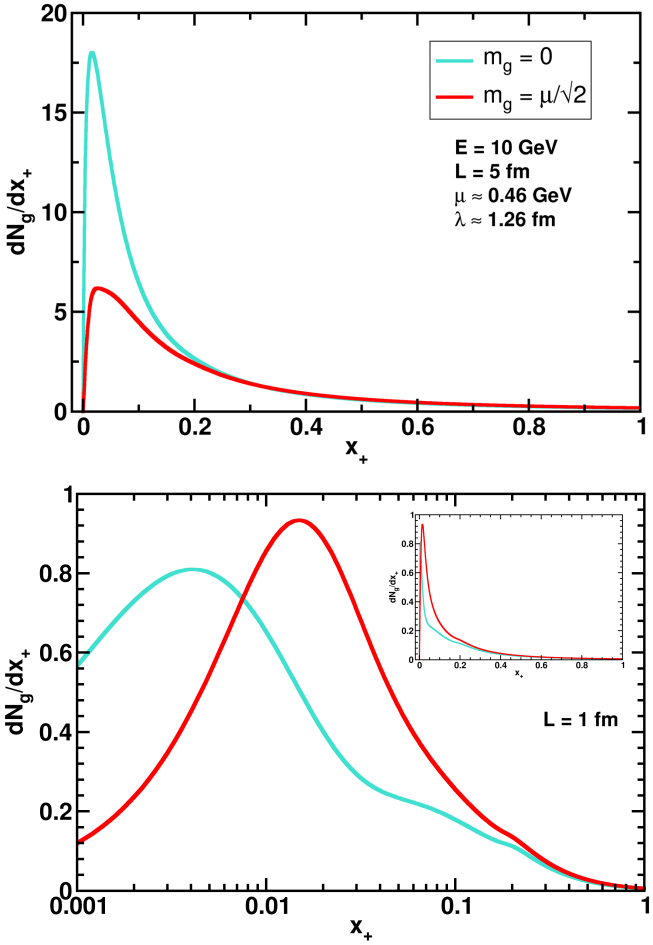

FIG. 5: Comparison of $dN_g/dx_E(x_E)$ from GLV and DGLV ($m_g = \mu/\sqrt{2}$) for a $E = 10$ GeV quark using typical RHIC medium parameters and $L = 5$ fm (top), $L = 1$ fm (bottom). Inset shows results on a linear scale for clarity. Note the *enhancement* of dN_g/dx at $L = 1$ fm for the massive case.

use of a Jacobian:

$$\frac{dN_g^J}{dx_E}(x_E) \equiv \int^{x_E E \sin(\theta_{\max})} dk_T \frac{dx_+}{dx_E} \frac{dN_g}{dx_+ dk_T}\big(x_+(x_E)\big), \tag{9}$$

$$\frac{dx_+}{dx_E} = \frac{1}{2}\left[1 + \left(1 - \left(\frac{k_T}{x_E E}\right)^2\right)^{-1}\right]. \tag{10}$$

Note the change in the upper limit of integration in Eq. (9) as dictated by the basic rules of calculus. The Jacobian, Eq. (10), is strictly greater than one and is singular as $k_T \to x_E E$; the competing effects between it and the numerically smaller $k_{\max}$ on dN_g^J/dx_E and energy loss will be discussed in further detail below.

IV. QUANTITATIVE COMPARISONS

We now wish to quantify the effects of the different x interpretations, $k_{\max}$ values, and gluon mass treatments on dN_g/dx and its derived quantities, such as $P(\epsilon)$, the medium parameter dN_g/dy extracted from R_{AA}, and the total radiated gluon multiplicity, $\langle N_g \rangle$. We will do so using five implementations of radiative energy loss; see Table II. In the first three calculations we use the $x = x_+$ interpretation and $\theta_{\max} = \pi/2$; in the first two we do not include the effect of the dx_+/dx_E Jacobian. In the first calculation we assume radiated gluons acquire a thermal mass on the order of the Debye scale, $m_g = \mu/\sqrt{2}$. The second calculation is the same as the first but with $m_g \to 0$. The third is the same as the second but includes the Jacobian transformation from x_+ to x_E. In the last two calculations we adopt the $x = x_E$ interpretation from the start: in the fourth we take $\theta_{\max} = \pi/2$ and the fifth $\theta_{\max} = \pi/4$.

We show in Fig. 4 top (bottom) the dramatic difference between the "equivalent" dN_g/dx_E spectra obtained using the two interpretations of x and taking $E = 10$ GeV, $L = 5$ fm ($L = 1$ fm), $\mu \approx 0.46$ GeV and $\lambda \approx 1.26$ fm as representative RHIC values. Also shown in the figure is the large reduction in dN_g/dx as $\theta_{\rm max}$ is reduced from $\pi/2$ to $\pi/4$. That reduction in the spectrum demonstrates the importance of large angle gluon emission despite the assumption of collinearity. Fig. 5 (top) shows the dramatic reduction in dN_g/dx with the introduction of a thermal gluon mass for the above parameter values; the bottom panel in the same figure shows that for shorter path lengths, such as $L = 1$ fm, the inclusion of a thermal mass for the radiated gluon can actually enhance the emission of bremsstrahlung radiation.

The only difference between the x_E and $x_+(x_E)$ curves, theoretically indistinguishable to lowest order in collinearity, in Fig. 4 comes from terms of $\mathcal{O}\big((k_T/x_E E)^2\big)$ and higher. Fig. 6 quantifies the reduction of the effect of these terms as we decrease $\theta_{\rm max}$ from 90° to 30°.

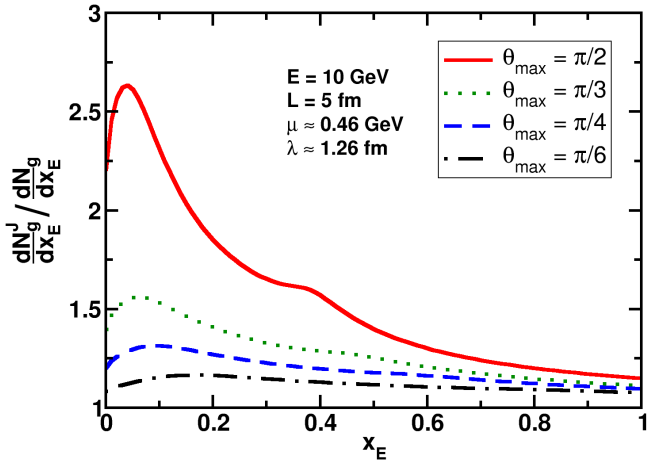

FIG. 6: Ratios of gluon spectra obtained from Eq. (9), $dN_g^J/dx_E(x_E)$, to that obtained from Eq. (2) with $x = x_E$, $dN_g/dx_E(x_E)$, as a function of x_E for different choices of $\theta_{\rm max}$. Smaller maximum opening angles produce a decreased sensitivity to the collinear approximation.

It is also worthwhile to consider the "apples-to-oranges" comparison of the $x_+(x_E)$ curve in Fig. 4 and the x_+, $m_g = 0$ curve in Fig. 5 (top). In particular, we observe that the former has a reduced peak height at $x \sim \mu/E$ but is larger for higher values of x. This generic behavior is due to a non-trivial interplay between the Jacobian, which always multiplies the dN_g/dx_+dk_T integrand by a number greater than 1, and the numerically reduced $k_{\rm max} = x_E E$ used in Eq. (9). Fig. 3 shows that the collinear approximation is better at larger values of x as demonstrated by the small values of $dN_g/dxdk_T$ at $k_T \sim k_{\rm max}$ compared to those at lower k_T. The Jacobian, though, introduces an integrable divergence at $k_T = x_E E$, so the $x_+(x_E)$ curve is systematically larger than the x_+ curve at larger values of x. Since the total gluon yield, $\langle N_g \rangle$, must be unmodified by a change in integration variables, the increased yield at larger x must come at the expense of gluon yield at smaller values of x; hence, the numerical reduction in $k_{\rm max}$ wins in this small x region. This redistribution of probability means that $\langle x \rangle$ from $x_+(x_E)$ is always greater than $\langle x \rangle$ from x_+. For any given set of medium parameters and path length, $\langle N_g \rangle$ must be the same for both the $x_+(x_E)$ and x_+ implementations; since $\langle x \rangle$ is always larger for the former, using $x_+(x_E)$ will always produce a smaller R_{AA} than x_+. For any given $\theta_{\rm max}$, $dN_g/dxdk_T$ with $x = x_+$ is integrated out to a larger $k_{\rm max}$ than for $x = x_E$. Therefore, the x_+ interpretation will always yield a smaller R_{AA} than the x_E interpretation. Using similar reasoning the x_E calculation with $\theta_{\rm max} = \pi/2$ will always generate a smaller R_{AA} than the x_E with $\theta_{\rm max} = \pi/4$ calculation. Based on these arguments we expect that the extracted medium parameter dN_g/dy will be ordered from smallest to largest according to $x_+(x_E)$, x_+, x_E with $\theta_{\rm max} = \pi/2$, x_E with $\theta_{\rm max} = \pi/4$. The dN_g/dy obtained via the statistical analysis (described below) and listed in Table I demonstrate exactly this ordering.

A crucial ingredient for any jet quenching calculation is $P(\epsilon)$, the probability distribution for the fraction of energy, ϵ, radiated by a high-p_T parton. Described above, $P(\epsilon)$ is obtained via a Poisson convolution of the single inclusive radiated gluon spectrum, dN_g/dx, assuming the independent emission of the multiple radiated gluons. $P(\epsilon)$ can be decomposed into discrete and continuous pieces,

$$P(\epsilon) = P^0\delta(\epsilon) + \tilde{P}(\epsilon) + P^1\delta(1-\epsilon). \qquad (11)$$

P^0 is the probability of radiating no gluons (and hence no energy loss) and is given by

$$P^0 = \exp(-\langle N_g \rangle). \qquad (12)$$

P^1 encodes the probability "leakage," the probability that the radiating parton loses a fraction of energy greater than unity, that results from the assumption of independent emissions used here. We show in Fig. 7 the $P(\epsilon)$ generated from four of the dN_g/dx curves investigated in this work (themselves displayed in Figs. 4 and 5): x_+ with $m_g = 0$, $x_+(x_E)$, x_E with $\theta_{\rm max} = \pi/2$, and x_E with $\theta_{\rm max} = \pi/4$. The ordering of the average fractional energy loss, $\langle \epsilon \rangle$, (represented by the vertical lines in Fig. 7) is consistent with the qualitative arguments of the previous paragraph. As noted previously $\langle N_g \rangle$ is identical for the x_+ and $x_+(x_E)$ models; hence, P^0 is also identical for the two. Previous evaluations of $P(\epsilon)$ using the x_+ interpretation approximated $dN_g/dx_+(x_+) \approx dN_g/dx_E(x_E)$. We find a systematic, though small, difference between the $\langle \epsilon \rangle$ from this approximation and that resulting from the correct transformation of dN_g/dx_+ to dN_g^J/dx_E; the modest variation in $P(\epsilon)$ also produces only a $\sim 10-20\%$ change in the extracted dN_g/dy. The continuous parts of $P(\epsilon)$, $\tilde{P}(\epsilon)$, have the expected ordering: from smallest to largest according to x_E with $\theta_{\rm max} = \pi/4$, x_E with $\theta_{\rm max} = \pi/2$, x_+.

This ordering follows simply from the integration of the $dN_g/dxdk_T$ curves out to successively larger $k_{\rm max}$. The non-trivial ordering of $\tilde{P}(\epsilon)$ for the x_+ and $x_+(x_E)$ interpretations shows explicitly the redistribution of probability from smaller to larger ϵ due to the combined effects of the Jacobian, Eq. (10), and the numerically reduced $k_{\rm max}$ of Eq. (9).

Ultimately, we wish to quantify the effects on extracted medium parameters of: (1) the two collinearly equivalent interpretations of x, (2) varying $k_{\rm max}$ (via $\theta_{\rm max}$), and (3) the thermal mass of the gluon. We will focus here on π^0 $R_{AA}(p_T)$ measurements obtained from the 5% most central Au+Au collisions at $\sqrt{s}$ = 200 AGeV [8]. We follow WHDG [32] in the implementation of energy loss: leading order pQCD-based production spectra for gluons and light quarks, followed by in-medium energy loss, and, finally, KKP fragmentation into pions. Initial state effects such as Cronin enhancement and shadowing are neglected; as such the p_T dependence of R_{AA} here is stronger than in works that better describe the trend of the data [26].

So far in this paper we have only discussed medium-induced gluon radiation, and for one set of R_{AA} calculations we continue to use purely radiative energy loss. However, it is known that for pQCD in the kinematic regimes appropriate to both RHIC and LHC, elastic scattering leads to a significant contribution to the total in-medium energy loss [31, 32]. Therefore, we will also calculate R_{AA} using convolved inelastic and collisional loss. We use the Braaten-Thoma calculation [59, 60] of the mean elastic energy loss and use the fluctuation-dissipation theorem to estimate the width of the elastic energy loss distribution [32]. We note that these assumptions are a poor approximation for RHIC conditions because the number of collisions is typically too small for the central limit theorem to apply. Hence, Gaussian distributions do not do a good job of representing the actual, highly skewed distributions involved; substantially improved results were derived in [56]. However, for the purposes of this paper we are not concerned with assessing the theoretical uncertainties resulting from the treatment of the elastic channel; this is a very interesting question in its own right.

For the radiative energy loss calculation, we include the full multi-gluon fluctuations through the Poisson convolution. We also account for path-length fluctuations due to parent parton production points and trajectories in the medium for both inelastic and collisional loss with an approximate implementation of Bjorken expansion [32]. A standard Glauber modeling of the medium with a diffuse Woods-Saxon nuclear density function is used [32]. Specifically, hard production is assumed to scale with binary collisions; the medium density is assumed to follow participant scaling. The strong coupling constant is held fixed at $\alpha_s = 0.3$. We use thermal field theory to relate $\mu = gT$ and $\lambda = 1/\rho\sigma$, with $\sigma \propto 1/\mu^2$ [32]. The only independent variable left is the single input parameter dN_g/dy, the rapidity density of gluons in the pure

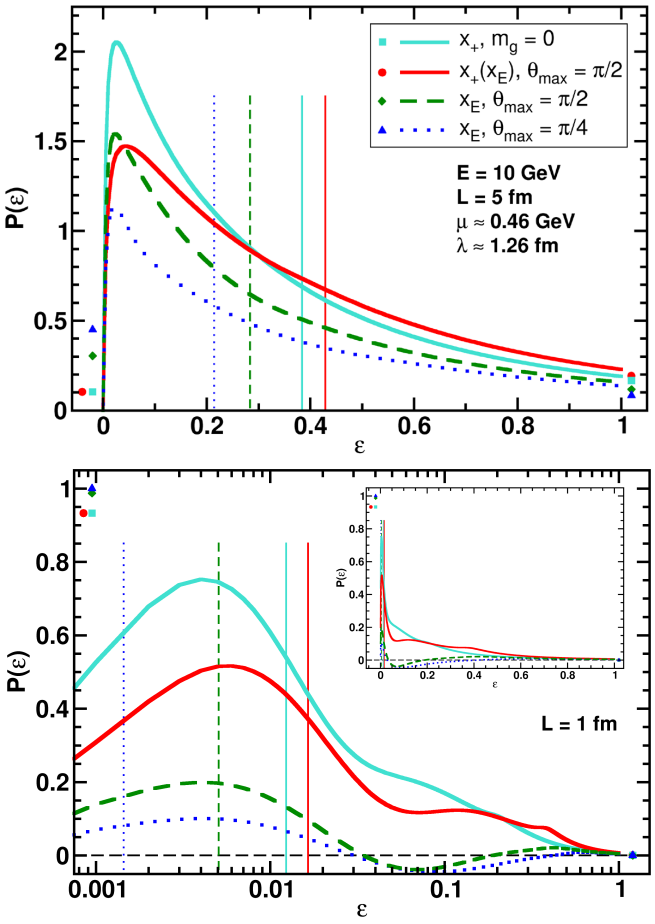

FIG. 7: Plots of $P(\epsilon)$ for a 10 GeV quark in typical RHIC conditions with $L = 5$ fm (top) and $L = 1$ fm (bottom). $P(\epsilon)$ obtained by convolving the single inclusive spectra dN_g/dx shown in Figs. 4 and 5. Vertical lines represent the $\langle\epsilon\rangle$ for each $P(\epsilon)$ distribution. Symbols represent the weight of the δ functions at $\epsilon = 0$ and $\epsilon = 1$. Inset shows results on a linear scale for clarity.

glue QGP assumed here (increasing dN_g/dy increases the medium density and decreases R_{AA}). The rigorous statistical analysis of [8, 9] was then used to determine the value and 1-σ uncertainty of dN_g/dy that yields a theoretical curve that "best fits" the data given the experimental statistical and systematic errors.

We show in Fig. 8 the PHENIX measurement of π^0 $R_{AA}(p_T)$ for the 5% most central collisions and the best fit curves to the data for the five different implementations of the radiative energy loss considered in this paper (see Table II) for both purely radiative energy loss (top) and convolved radiative and elastic loss (bottom). We note that, when compared at similar centrality bins, the STAR measurements of [61] $\pi^+ + \pi^-$ R_{AA} systematically differ from the shown PHENIX π^0 R_{AA} [8] by as much as $\sim 50\%$. Such a discrepancy represents a potential source of additional systematic uncertainty in extracted medium properties that we do not attempt to evaluate here.

The results in Fig. 8 indicate that the extracted dN_g/dy values for the massive ($m_g = \mu/\sqrt{2}$) and massless ($m_g = 0$) emitted gluon cases are quite similar despite the large differences in dN_g/dx for large path lengths, Fig. 5 (top). As we have shown this behavior is due to the interaction of the effects of a thermal gluon mass on the coherence length and the radiation kernel. As the path length decreases, the difference between the massive and massless integrated dN_g/dx decreases until eventually the massive distribution exceeds the massless one. For central RHIC collisions the results shown in Fig. 5 (bottom) indicate this path length is ~ 1 fm. As noted in [25] physical observables are quite sensitive to the specific numerical choice of the IR cutoff taken when used to approximate the inclusion of a thermal mass for the radiated gluon. The lack of sensitivity to the particular choice of gluon mass seen in this paper is a pleasant surprise. For the convolved energy loss, the extracted medium density is consistent for massive and massless radiated gluons. For identical values of dN_g/dy the massless case yields a smaller R_{AA}; that the extracted medium parameter is consistent is likely due to the statistical analysis trading off goodness of fit in the normalization of R_{AA} for slightly different p_T dependencies.

Addressing the primary goal of this paper, we observe from the results in Fig. 8 that the extracted values of dN_g/dy for the radiative only energy loss models $x_+(x_E)$; x_E, $\theta_{\rm max} = \pi/2$; and x_E, $\theta_{\rm max} = \pi/4$ vary almost by 200%. It cannot be overemphasized that the first two cases—for which dN_g/dy varies by $\sim 100\%$—are *exactly equivalent* under the collinear assumption used in the energy loss derivation. As discussed previously, for any particular $\theta_{\rm max}$, $x_+(x_E)$ produces the smallest R_{AA}. Thus, $x_+(x_E)$ with $\theta_{\rm max} = \pi/2$ represents a lower bound on R_{AA} for fixed medium parameters. Unfortunately, it is not possible to rigorously define an upper bound to the theoretical uncertainty on R_{AA} since decreasing $\theta_{\rm max} \to 0$ makes $R_{AA} \to 1$. We choose the values of observables calculated from the x_E with $\theta_{\rm max} = \pi/4$ implementation as a working definition of the upper bound. We consider this $\theta_{\rm max}$ as representing a reasonable $\mathcal{O}(1)$ variation of the coefficient of the k_T cutoff that necessarily increases R_{AA} for a given medium density; the surprise, of course, is just how sensitive R_{AA} is to such a variation of the cutoff. It is worth noting that the larger dN_g/dy values extracted using the radiative energy loss only models are difficult to reconcile with known RHIC dN_{ch}/dy multiplicities [62].

An important question that must be addressed is whether or not the sensitivity of extracted medium properties to variations in the implementation of the collinear approximation decreases with increasing radiating parton energy. To address this question, we show in Fig. 9 a "toy model" quark partonic $R_{AA}(p_T)$ calculation for $L = 5$ fm fixed path length and typical RHIC medium parameters used above. The sensitivity of the partonic $R_{AA}(p_T)$ to different implementations of the collinear approximation

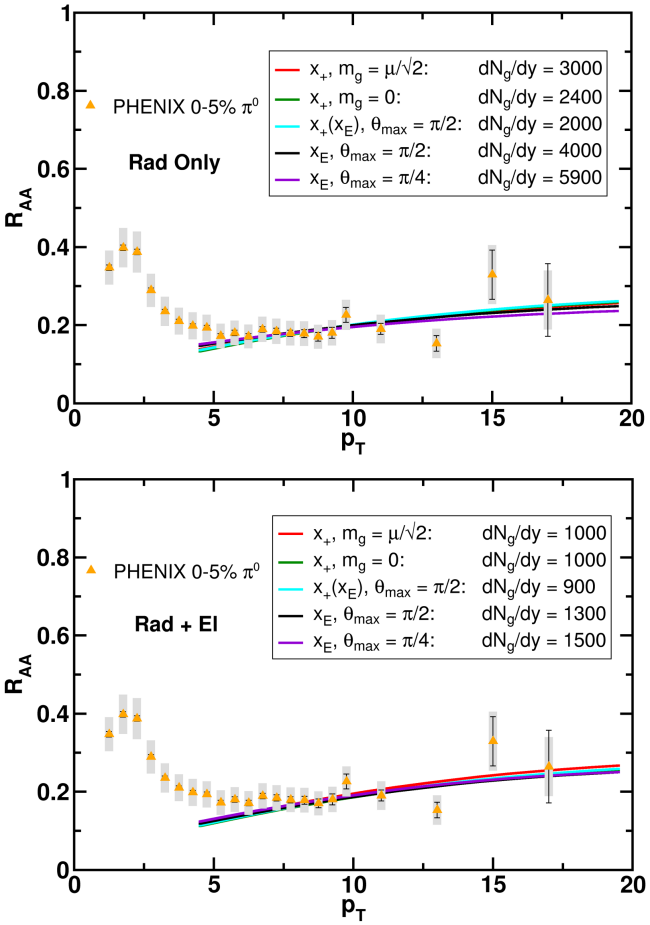

FIG. 8: The "best fit" curves of the five models discussed in the text to PHENIX measurements of the 5% most central π^0 R_{AA} [8]: top–including only radiative energy loss, bottom–including both radiative and collisional energy loss. Fits performed using the methods of [8, 9]. Uncorrelated errors are represented by bars whereas correlated errors are shown as grey boxes, and there is an overall scale uncertainty of $\pm 12\%$ not shown.

decreases with increasing parton energy. For example, the $\simeq 100\%$ difference at 5 GeV between the collinearly equivalent $x_+(x_E)$ and x_E interpretations decreases to $\simeq 10\%$ at 200 GeV. But, we observe that the number of emitted gluons, $\langle N_g \rangle$, remains sensitive to the uncertainties introduced by the collinear approximation; the $\sim$ factor of 2 difference in $\langle N_g \rangle$ shown in Fig. 9 is nearly energy independent.

The convergence of the ratios of $R_{AA}(p_T)$ with increasing energy can be understood at least partly as a consequence of the small x pileup in dN_g/dx. For an energy loss model with $P(\epsilon)$ and a power law production spectrum $dN/dp_T \propto p_T^{-(n+1)}$ we have that $R_{AA}(p_T) \simeq \int (1-\epsilon)^n P(\epsilon; p_T) d\epsilon$. Then for any two models, say 1 and 2,

$$\frac{R^1_{AA}}{R^2_{AA}}(p_T) \simeq 1 - n\Big(\langle \epsilon_1 \rangle(p_T) - \langle \epsilon_2 \rangle(p_T)\Big), \qquad (13)$$

and the ratio of modification factors automatically approaches 1 as the mean energy loss decreases with increasing p_T. On the other hand, the constancy of $\langle N_g \rangle$ in p_T is due to the surprising energy independence of the area under the peak in the dN_g/dx distribution. As the energy increases, the distribution becomes more sharply peaked, and its normalization becomes more and more dominated by this energy-independent area.

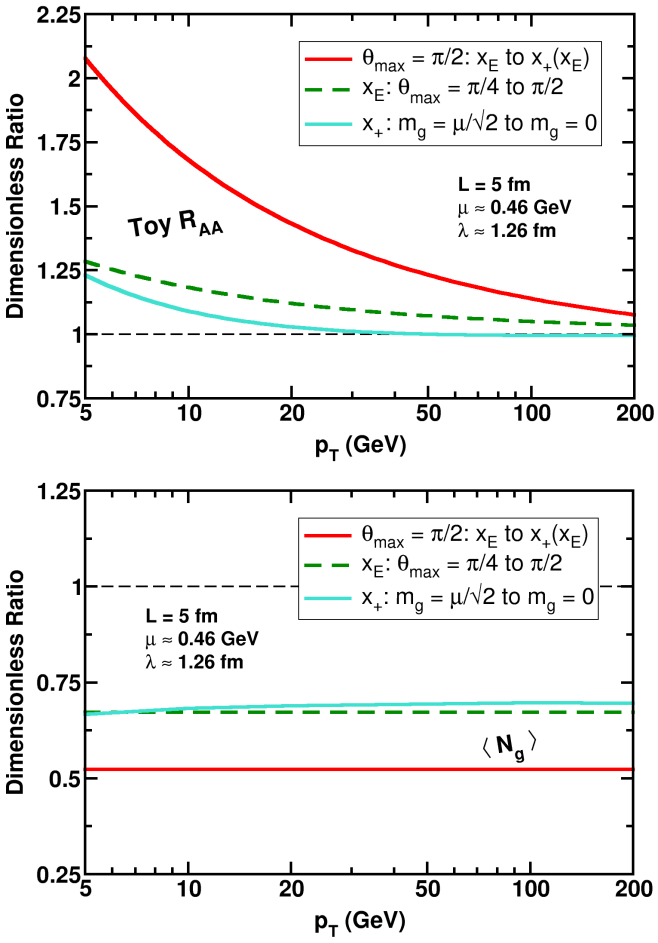

FIG. 9: Ratios of a toy R_{AA} model (top) and ratios of the average number of emitted gluons, $\langle N \rangle$, (bottom) as a function of parent quark energy for the five models discussed in the text. Collinear and gluon mass effects die out with increasing energy for the toy R_{AA} but do not for $\langle N \rangle$.

V. CONCLUSIONS

In our introduction, we laid out the numerous approximations used in deriving the opacity expansion energy loss formulae. In one form or another, these assumptions are at the foundation of the four energy loss calculations that are frequently compared to RHIC data. In particular, these calculations all rely on the lowest order term in a collinear expansion, where the small parameter is k_T/xE. Unfortunately, we have found that the opacity expansion energy loss kernel $dN_g/dxdk_T$ drastically violates the collinear approximation for small values of x, the region of x most important for computing many observables including the leading particle suppression and the average number of emitted bremsstrahlung gluons. While we did not explicitly check this violation for the other energy loss formalisms, it is highly likely they also will be similarly strongly affected by the large angle radiation that, by assumption of collinearity, is not under theoretical control.

To leading order in collinearity, the two common definitions of x used in energy loss calculations—$x = x_+$, the fraction of light-cone plus momentum, and $x = x_E$, the fraction of energy taken away by the radiated gluon—are equivalent. We found that for RHIC conditions, the "best fit" medium density dN_g/dy extracted using these two different, but collinearly equivalent, definitions of x varies by a factor of ~ 2.

While one may use the $x_+(x_E)$ interpretation with $\theta_{\rm max} = \pi/2$ as a natural lower bound for the systematic theoretical uncertainty of R_{AA}, the upper bound is less obvious. We take the results from the x_E and $\theta_{\rm max} = \pi/4$ as a working definition; in this case the extracted medium density increases another $\sim 50\%$ over the x_E and $\theta_{\rm max} = \pi/2$ model. We note that there is no sense of a "central value" or Gaussian distribution for this uncertainty band: the rigorous notion of a "best" interpretation of x or the "correct" UV cutoff for the lowest order collinear results does not exist prior to a calculation based on a more exact analytic derivation.

The uncertainties we quote decrease significantly when elastic energy loss is included although the effects of uncertainty in the collisional channel were not considered here. While the leading particle R_{AA} appears to suffer less systematic uncertainty at LHC energies, the uncertainty in other observables, such as the mean number of emitted gluons, are energy independent. Finally, the effect of a thermal gluon mass on the extracted medium density is surprisingly small due to non-trivial coherence effects. This last result implies that the specifics of the short path length energy loss behavior are very important; future work should, therefore, go beyond the $L \gg \lambda$ approximation.

One of the great debates over the past several years has been the so-called "discrepancy" of extracted medium parameters from the four energy loss models. An oversimplified description would be that the density found when comparing AMY, GLV, and HT to data is reasonably consistent while that found from BDMPS is a factor $\sim 2-3$ times larger [8, 9, 35]. It is natural and right to begin any calculation with assumptions about the relevant and irrelevant physics of the problem. However, that the four models include and exclude vastly different physics implies to us that any consistency found must be considered coincidental, even surprising. We see the path forward not in teasing out the origins of the extracted difference but in finding observables that can falsify the basic assumptions about the relevant physics

of the quark gluon plasma. Is the medium strongly or weakly coupled? What are its degrees of freedom? If energy loss is perturbative, are parton interactions with the medium better approximated by many soft scatterings or a few hard ones? In order to answer these questions we must have not only well-controlled experiments but well-controlled theories. It is, thus, imperative that quantitative estimates be made of the systematic uncertainty introduced into theoretical results from the simplifying assumptions—distinct from the physics assumptions—made in the calculation.

As discussed previously there is no notion of "one standard deviation" of theoretical uncertainty associated with the collinear approximation. Moreover, we have not quantified the consequences of the collinear approximation for the other three energy loss models, although this is both an extremely interesting and clearly important problem. Nevertheless, we strongly suspect that should this uncertainty be quantified for the other models, then the different values of medium density so far extracted from data would be mutually consistent within the systematic theoretical uncertainties. As we have shown in this work, any hope for a quantitative extraction of medium density from high-p_T physics at RHIC using the GLV formalism requires a far more careful treatment of non-collinear radiation; this is almost certainly true for the AMY, BDMPS-Z-ASW, and HT formalisms, too. It is interesting that at LHC the leading particle suppression seems a rather collinearly safe observable whereas the average number of emitted gluons and the spectrum of soft gluons is not. This suggests that—at our current level of theoretical understanding—leading particle observables and jets measured using narrower cones may provide more sensitive tests of jet quenching at the LHC than, e.g., full jet reconstruction with large cones.

The authors wish to thank Miklos Gyulassy, Yuri Kovchegov, and the members of the TECHQM Collaboration for valuable discussions; in particular we thank Ulrich Heinz and Urs Wiedemann for their help in elucidating the differences between the x_+ and x_E definitions. Additionally the authors thank Jamie Nagle for quantitatively extracting dN_g/dy from PHENIX data and the calculations presented in this work. We also thank Ulrich Heinz for reading and commenting on the manuscript. WAH thanks the Aspen Center for Physics for support during his stay. This work was supported by the Office of Nuclear Physics in the Office of Science of the U.S. Department of Energy under Grant Nos. DE-FG02-05ER41377 and DE-FG02-86ER40281.

[1] M. Gyulassy and L. McLerran, Nucl. Phys. **A750**, 30 (2005), arXiv:nucl-th/0405013.
[2] W. A. Horowitz and M. Gyulassy, Phys. Lett. **B666**, 320 (2008), arXiv:0706.2336.
[3] M. Gyulassy and X. Wang, Nucl. Phys. **B420**, 583 (1994), arXiv:nucl-th/9306003.
[4] C. P. Herzog, A. Karch, P. Kovtun, C. Kozcaz, and L. G. Yaffe, JHEP **07**, 013 (2006), arXiv:hep-th/0605158.
[5] S. S. Gubser, Phys. Rev. **D74**, 126005 (2006), arXiv:hep-th/0605182.
[6] M. Gyulassy, Lect. Notes Phys. **583**, 37 (2002), arXiv:nucl-th/0106072.
[7] M. Gyulassy, P. Levai, and I. Vitev, Phys. Lett. **B538**, 282 (2002), arXiv:nucl-th/0112071.
[8] A. Adare et al. (PHENIX), Phys. Rev. **C77**, 064907 (2008), arXiv:0801.1665.
[9] A. Adare et al. (PHENIX), Phys. Rev. Lett. **101**, 232301 (2008), arXiv:0801.4020.
[10] W. A. Horowitz and Y. V. Kovchegov, Phys. Lett. **B680**, 56 (2009), arXiv:0904.2536.
[11] J. L. Nagle (2009), arXiv:0907.2707.
[12] S. S. Adler et al. (PHENIX), Phys. Rev. **C75**, 024909 (2007), arXiv:nucl-ex/0611006.
[13] G. Lin (STAR), J. Phys. **G35**, 104046 (2008).
[14] B. I. Abelev et al. (STAR), Phys. Rev. **C80**, 024905 (2009), arXiv:0907.2721.
[15] S. Afanasiev et al. (PHENIX) (2009), arXiv:0903.4886.
[16] A. Adare et al. (PHENIX), Phys. Rev. Lett. **98**, 172301 (2007), arXiv:nucl-ex/0611018.
[17] B. I. Abelev et al. (STAR), Phys. Rev. Lett. **98**, 192301 (2007), arXiv:nucl-ex/0607012.
[18] A. Adare et al. (PHENIX), Phys. Rev. Lett. **103**, 082002 (2009), arXiv:0903.4851.
[19] G. Wang (STAR), J. Phys. **G35**, 104107 (2008), arXiv:0804.4448.
[20] B. I. Abelev et al. (STAR) (2009), arXiv:0904.1722.
[21] W. Horowitz, Nucl. Phys. **A783**, 543 (2007), arXiv:nucl-th/0610024.
[22] S. Wicks, W. Horowitz, M. Djordjevic, and M. Gyulassy, Nucl. Phys. **A783**, 493 (2007), arXiv:nucl-th/0701063.
[23] A. Dainese, C. Loizides, and G. Paic, Eur. Phys. J. **C38**, 461 (2005), arXiv:hep-ph/0406201.
[24] K. Eskola, H. Honkanen, C. Salgado, and U. Wiedemann, Nucl. Phys. **A747**, 511 (2005), arXiv:hep-ph/0406319.
[25] R. Baier, Y. L. Dokshitzer, A. H. Mueller, and D. Schiff, JHEP **09**, 033 (2001), arXiv:hep-ph/0106347.
[26] M. Gyulassy, P. Levai, and I. Vitev, Nucl. Phys. **B571**, 197 (2000), arXiv:hep-ph/9907461.
[27] M. Gyulassy, P. Levai, and I. Vitev, Nucl. Phys. **B594**, 371 (2001), arXiv:nucl-th/0006010.
[28] U. A. Wiedemann, Nucl. Phys. **B588**, 303 (2000), arXiv:hep-ph/0005129.
[29] M. Djordjevic and M. Gyulassy, Nucl. Phys. **A733**, 265 (2004), arXiv:nucl-th/0310076.
[30] M. Djordjevic and U. W. Heinz, Phys. Rev. Lett. **101**, 022302 (2008), arXiv:0802.1230.
[31] M. G. Mustafa, Phys. Rev. **C72**, 014905 (2005), arXiv:hep-ph/0412402.
[32] S. Wicks, W. Horowitz, M. Djordjevic, and M. Gyulassy, Nucl. Phys. **A784**, 426 (2007), arXiv:nucl-th/0512076.
[33] H. Zhang, J. F. Owens, E. Wang, and X. Wang, Phys. Rev. Lett. **98**, 212301 (2007), arXiv:nucl-

th/0701045.
[34] G.-Y. Qin et al., Phys. Rev. Lett. **100**, 072301 (2008), arXiv:0710.0605.
[35] S. A. Bass et al., Phys. Rev. **C79**, 024901 (2009), arXiv:0808.0908.
[36] R. Baier, Y. L. Dokshitzer, A. H. Mueller, S. Peigne, and D. Schiff, Nucl. Phys. **B483**, 291 (1997), arXiv:hep-ph/9607355.
[37] R. Baier, Y. L. Dokshitzer, A. H. Mueller, S. Peigne, and D. Schiff, Nucl. Phys. **B484**, 265 (1997), arXiv:hep-ph/9608322.
[38] B. G. Zakharov, JETP Lett. **63**, 952 (1996), arXiv:hep-ph/9607440.
[39] B. G. Zakharov, JETP Lett. **65**, 615 (1997), arXiv:hep-ph/9704255.
[40] B. G. Zakharov, Phys. Atom. Nucl. **61**, 838 (1998), arXiv:hep-ph/9807540.
[41] U. A. Wiedemann, Nucl. Phys. **B582**, 409 (2000), arXiv:hep-ph/0003021.
[42] C. A. Salgado and U. A. Wiedemann, Phys. Rev. Lett. **89**, 092303 (2002), arXiv:hep-ph/0204221.
[43] N. Armesto, C. A. Salgado, and U. A. Wiedemann, Phys. Rev. **D69**, 114003 (2004), arXiv:hep-ph/0312106.
[44] C. A. Salgado and U. A. Wiedemann, Phys. Rev. **D68**, 014008 (2003), arXiv:hep-ph/0302184.
[45] N. Armesto, C. A. Salgado, and U. A. Wiedemann, Phys. Rev. Lett. **94**, 022002 (2005), arXiv:hep-ph/0407018.
[46] X. Guo and X. Wang, Phys. Rev. Lett. **85**, 3591 (2000), arXiv:hep-ph/0005044.
[47] X. Wang and X. Guo, Nucl. Phys. **A696**, 788 (2001), arXiv:hep-ph/0102230.
[48] B.-W. Zhang and X. Wang, Nucl. Phys. **A720**, 429 (2003), arXiv:hep-ph/0301195.
[49] A. Majumder, E. Wang, and X. Wang, Phys. Rev. Lett. **99**, 152301 (2007), arXiv:nucl-th/0412061.
[50] P. Arnold, G. D. Moore, and L. G. Yaffe, JHEP **11**, 001 (2000), arXiv:hep-ph/0010177.
[51] P. Arnold, G. D. Moore, and L. G. Yaffe, JHEP **11**, 057 (2001), arXiv:hep-ph/0109064.
[52] S. Jeon and G. D. Moore, Phys. Rev. **C71**, 034901 (2005), arXiv:hep-ph/0309332.
[53] S. Turbide, C. Gale, S. Jeon, and G. D. Moore, Phys. Rev. **C72**, 014906 (2005), arXiv:hep-ph/0502248.
[54] A. Kovner and U. Wiedemann, in *Quark gluon plasma 3*, edited by R. Hwa and X. Wang (World Scientific, 2003), pp. 192–248, arXiv:hep-ph/0304151.
[55] S. Wicks (2008), arXiv:0804.4704.
[56] S. Wicks, Ph.D. thesis, Columbia University (2008).
[57] W. A. Horowitz and B. A. Cole, in preparation.
[58] M. Gyulassy, P. Levai, and I. Vitev, Phys. Rev. Lett. **85**, 5535 (2000), arXiv:nucl-th/0005032.
[59] E. Braaten and M. H. Thoma, Phys. Rev. **D44**, 1298 (1991).
[60] E. Braaten and M. H. Thoma, Phys. Rev. **D44**, 2625 (1991).
[61] B. I. Abelev et al. (STAR), Phys. Lett. **B655**, 104 (2007), arXiv:nucl-ex/0703040.
[62] B. Back et al. (PHOBOS), Phys. Rev. **C65**, 061901 (2002), arXiv:nucl-ex/0201005.